



GPU Computing in Economics

Eric M. Aldrich

Department of Economics, University of California, Santa Cruz, USA

Contents

1. Introduction	557
2. Basics of GPGPU Computing	560
2.1 Hardware Architecture	560
2.1.1 Processing Hardware	560
2.1.2 Memory	561
2.1.3 Scaling	562
2.2 Algorithmic Design	562
2.3 Software	564
3. A Simple GPGPU Example	565
3.1 Matlab	567
3.2 C++	569
3.3 CUDA C	572
3.4 Thrust	577
4. Example: Value Function Iteration	580
4.1 Model	580
4.2 Solution	582
4.3 Results	582
5. Example: A General Equilibrium Asset Pricing Model with Heterogeneous Beliefs	586
5.1 Model	587
5.1.1 First-Order Conditions	588
5.2 Solution	589
5.3 Results	591
6. The Road Ahead	593
6.1 NVIDIA Kepler and CUDA 5	594
6.2 Intel Phi	595
6.3 OpenACC	595
7. Conclusion	596
References	597



1. INTRODUCTION

The first parallel computing systems date back to the 1960s and 1970s, but were limited to specialty machines with limited accessibility and distribution. Examples of early systems include the Burroughs D825 and the CDC 6600. Early development of parallel

architectures led to a taxonomy of systems that defined the method by which instructions operate on data elements as well as the method of sharing memory across processing units. Two broad classifications for parallel instruction/data operation include Single-Instruction Multiple-Data (SIMD) and Multiple-Instruction Multiple-Data. In the former, SIMD, identical instructions operate on distinct data elements in a lockstep, parallel fashion. MIMD, as the name suggests, allows for more flexible design of operations across parallel data elements. These broad parallel specifications can be further dichotomized into shared and distributed memory models; shared-memory systems allowing all processor cores access to the same memory bank where the data resides, while distributed memory maintains distinct memory units for each processor (requiring movement of data elements among memory units). An overview of these architectures can be found in [Dongarra and van der Steen \(2012\)](#).

Advances in computational hardware and their reduction in cost led to a surge in distributed parallel computing in the 1990s. During this period, single-core microprocessor speeds were increasing at such a fast rate that powerful parallel computing systems were easily designed by connecting a large number of compute nodes, each with an individual core. Standards such as the Message Passing Interface (MPI) were developed to allow communication among the distributed nodes. The first Beowulf cluster, introduced in 1994, was an example of such a system. It is a model that has been widely utilized to the present day and which has been largely responsible for making parallel computing available to the masses. However, in the early 2000s, microprocessors became increasingly limited in terms of speed gains and much of the focus of system design in the computing industry shifted toward developing multicore and multiprocessor Central Processing Units (CPUs).

Somewhat independently, the market for high-end graphics in the entertainment industry led to the development of many-core Graphical Processing Units (GPUs) in the 1990s. These graphics cards were inherently SIMD, performing identical floating point instructions on millions of pixels, and so they were designed to have numerous individual processing units with high arithmetic intensity—many transistors dedicated to floating point, arithmetic operations, but very few dedicated to memory management and control flow. The result was that consumer-grade GPUs had high arithmetic power for a very low cost.

Some time after the turn of the millennium, a number of computational scientists, recognizing the low cost and low power consumption per unit of arithmetic power (typically measured in FLOPS—Floating Point Operations Per Second), began using GPUs as parallel hardware devices for solving scientific problems. Early examples spanned the fields of computer science ([Kruger and Westermann \(2002\)](#) and [Purcell et al. \(2002\)](#)), fluid dynamics ([Harris et al. \(2003\)](#)), bioinformatics ([Charalambous et al. \(2005\)](#)), and

molecular dynamics (Stone et al. (2007)), to name a few. In each case scientists recognized similarities between their algorithms and the work of rendering millions of graphical pixels in parallel. In response to the uptake of GPU computing in broad scientific fields, NVIDIA released a set of software development tools in 2006, known as Compute Unified Device Architecture (CUDA—http://www.nvidia.com/object/cuda_home_new.html) (NVIDIA (2012a)). The intention of CUDA was to facilitate higher-level interactions with graphics cards and to make their resources accessible through industry standard languages, such as C and C++. This facilitated a new discipline of General Purpose GPU (GPGPU) computing, with a number of subsequent tools that have been developed and released by a variety of hardware and software vendors.

The uptake of GPGPU computing in Economics has been slow, despite the need for computational power in many economic problems. Recent examples include Aldrich (2011), which solves a general equilibrium asset pricing model with heterogeneous beliefs, Aldrich et al. (2011), which solves a dynamic programming problem with value function iteration, Creal (2012), which solves for the likelihood for affine stochastic volatility models, Creel and Kristensen (2011), which explores the properties of indirect likelihood estimators, Durham and Geweke (2011) and Durham and Geweke (2012), which develop a parallel algorithm for sequential Monte Carlo, Dziubinski and Grassi (2012), which replicates the work of Aldrich et al. (2011) with Microsoft's C++Amp library (<http://msdn.microsoft.com/en-us/library/vstudio/hh265137.aspx>) (Microsoft (2012)), Fulop and Li (2012), which uses sequential Monte Carlo and resampling for parameter learning, and Lee et al. (2010a), which shows how to use GPUs for Markov Chain Monte Carlo and sequential Monte Carlo simulation. The objective of this paper will be to demonstrate the applicability of massively parallel computing to economic problems and to highlight situations in which it is most beneficial and of little use.

The benefits of GPGPU computing in economics will be demonstrated via two specific examples with very different structures. The first, a basic dynamic programming problem solved with value function iteration, provides a simple framework to demonstrate the parallel nature of many problems and how their computational structure can be quickly adapted to a massively parallel framework. The second example, a general equilibrium asset pricing model with heterogeneous beliefs, uses an iterative procedure to compute optimal consumption allocations for a finite time horizon T . This example experiences great gains from GPU parallelism, with the GPU allowing the solution of far longer time horizons than would be feasible on a CPU. A substantial portion of this paper will also be dedicated to introducing specific hardware and software platforms that are useful for GPGPU computing, with the end objective to help researchers in economics to not only become familiar with the requisite computing tools, but also to design and adapt algorithms for use on GPU parallel hardware.

The structure of this paper will be as follows. [Section 2](#) will introduce the basic concepts of GPGPU computing and [Section 3](#) will illustrate these concepts in the context of a very simple example. [Sections 4](#) and [5](#) will consider the dynamic programming and heterogeneous beliefs examples mentioned above, demonstrate how the solutions can be parallelized, and report timing results. [Section 6](#) will discuss recent developments in parallel computing and will offer a glimpse of the future of the discipline and potential changes for economic computing. [Section 7](#) will conclude.



2. BASICS OF GPGPU COMPUTING

This section will introduce the basics of GPU hardware, software, and algorithms. The details of this section will be useful for understanding the specific applications in [Sections 3–5](#).

2.1 Hardware Architecture

Understanding the basics of GPU architecture facilitates the design of massively parallel software for graphics devices. For illustrative purposes, this section will often reference the specifications of an NVIDIA Tesla C2075 GPU ([NVIDIA \(2011\)](#)), a current high-end GPU intended for scientific computing.

2.1.1 Processing Hardware

GPUs are comprised of dozens to thousands of individual processing cores. These cores, known as thread processors, are typically grouped together into several distinct multiprocessors. For example, the Tesla C2075 has a total of 448 cores, aggregated into groups of 32 cores per multiprocessor, yielding a total of 14 multiprocessors. Relative to CPU cores, GPU cores typically:

- Have a lower clock speed. Each Tesla C2075 core clocks in at 1.15 GHz, which is roughly 30–40% the clock speed of current CPUs (e.g., the current fastest desktop and server CPUs made by Intel are the 3.6 GHz i7-3820 ([Intel Corporation \(2013a\)](#)) and the 2.67 GHz E7-8837 ([Intel Corporation \(2011\)](#)), respectively).
- Dedicate more transistors to arithmetic operations and fewer to control flow and data caching.
- Have access to less memory. A Tesla C2075 has 6 gigabytes of global memory, shared among all cores.

Clearly, where GPU cores are lacking in clock speed and memory access, they compensate with the sheer quantity of compute cores. For this reason, they are ideal for computational work that has a high arithmetic intensity: many arithmetic operations for each byte of memory transfer/access. It is important to note that this does not mean that every problem which requires high arithmetic intensity will benefit from GPU parallelization; in addition

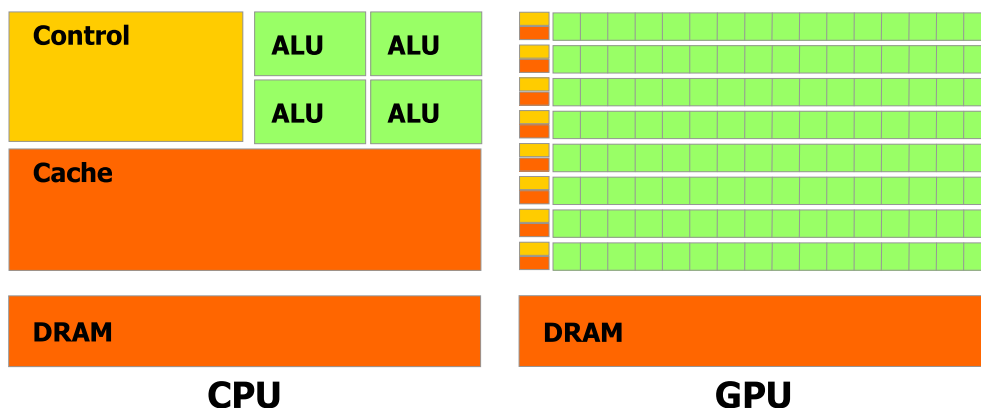


Figure 1 Schematic diagram of CPU and GPU processors, taken from Section 1.1 of [NVIDIA \(2012a\)](#). The diagram illustrates how traditional CPUs dedicate more transistors to memory and control (yellow and orange blocks) and fewer to floating point operations (green blocks), relative to GPUs. (For interpretation of the references to color in this figure legend, the reader is referred to the web version of this book.)

to arithmetic intensity, the problem must be divisible into hundreds or thousands of data elements, each requiring an almost identical sequence of computational operations. Where these latter conditions are not met, a heterogeneous CPU environment, using OpenMP or MPI, may be ideal.

[Figure 1](#) depicts a schematic diagram of CPU and GPU architectures, taken from Section 1.1 of [NVIDIA \(2012a\)](#). The diagram illustrates the allocation of transistors for each type of microprocessor. In particular, traditional CPUs dedicate relatively more transistors to memory and control flow (the yellow and orange blocks) and fewer to algorithmic logic units (ALUs) which perform floating point computations (the green blocks). GPUs, on the other hand, dedicate many more transistors to ALUs and far fewer to memory and control.

2.1.2 Memory

There is a distinction between CPU memory and GPU memory, the former being referred to as “host” memory and the latter as “device” memory. GPU instructions can only operate on data objects that are located in device memory—attempting to pass a variable in host memory as an argument to a kernel would generate an error. Thus, GPU software design often necessitates the transfer of data objects between host and device memory.

Currently, memory transfers between host and device occur over a PCIe v2.0 $\times 16$ interface, which for an NVIDIA Tesla C2075 GPU translates into a maximum data

transfer bandwidth of 8 gigabytes per second ([PCI-SIG \(2006\)](#)). This is approximately 1/4th the bandwidth between common configurations of host memory and CPU at the present date. For this reason it is crucial to keep track of host-device memory transfers, since programs that require large amounts of CPU-GPU data transfer relative to the number of floating point operations performed by the GPU can experience severe limits to performance.

The architecture of GPU memory itself is also important. While all GPU cores share a bank of global memory, portions of the global memory are partitioned for shared use among cores on a multiprocessor. Access to this shared memory is much faster than global memory. While these issues can be beneficial to the design of parallel algorithms, the intricacies of GPU memory architecture are beyond the scope of this paper. A detailed treatment of GPU memory architecture and use can be found in [NVIDIA \(2012a\)](#).

2.1.3 Scaling

Two notions of scalability are relevant to GPU computing: scaling within GPU devices and across GPU devices. One powerful feature of GPU computing is that it automatically handles within-device scaling when software is moved to GPU devices with differing numbers of cores. GPU interfaces (discussed below) allow software designers to be agnostic about the exact architecture of a stand-alone GPU—the user does nothing more than designate the size of thread blocks (described in [Section 2.2](#)), which are then allocated to multiprocessors by the GPU scheduler. Although different block sizes are optimal for different GPUs (based on number of processing cores), it is not requisite to change block sizes when moving code from one device to another. The upshot is that the scheduler deals with scalability so that issues related to core count and interaction among cores on a specific device are transparent to the user. This increases the portability of massively parallel GPU software.

GPU occupancy is a measure of the number of threads concurrently scheduled on an individual core and is related to within-GPU scaling. While the number of total threads can be less than the number of cores, GPU devices achieve their best performance results when there are many threads concurrently scheduled on each core. Each device has a limit (which varies by device) to the number of threads which can be scheduled on a multiprocessor and occupancy is the ratio of actual scheduled thread warps (defined below) to the maximum number possible ([NVIDIA \(2012a\)](#)).

Scalability across GPU devices is achieved in a more traditional manner, using OpenMP or MPI.

2.2 Algorithmic Design

For a given computational program, there is no guarantee that any portion of the program may be computed in parallel. In practice, most algorithms have some fraction of

instructions which must be performed sequentially, and a remaining fraction which may be implemented in parallel. Amdahl's Law (Amdahl (1967)) states that if a fraction P of a program can be executed in parallel, the theoretical maximum speedup of the program with N processing cores is

$$S(N) = \frac{1}{(1 - P) + \frac{P}{N}}. \quad (1)$$

The intuition behind Amdahl's Law is the following. If a serial version of an algorithm takes 1 unit of time to execute, a fraction $(1 - P)$ of a parallel algorithm will execute in the same time as its serial counterpart, whereas a fraction P will run in $\frac{P}{N}$ units of time (because it can be run in parallel on N cores). Dividing 1 unit of time by the parallel compute time yields the possible speedup in Eq. (1). A crucial step in GPU computing is determining which portion of an algorithm can be executed in parallel.

Kernels and threads are the fundamental elements of GPU computing problems. Kernels are special functions that comprise a sequence of instructions that are issued in parallel over a user specified data structure (e.g., the fraction of instructions P mentioned above, such as performing a routine on each element of a vector). Thus, a kernel typically comprises only a portion of the total set of instructions within an algorithm. Each data element and corresponding kernel comprise a thread, which is an independent problem that is assigned to one GPU core.

Just as GPU cores are grouped together as multiprocessors, threads are grouped together in user-defined groups known as blocks. Thread blocks execute on exactly one multiprocessor, and typically many thread blocks are simultaneously assigned to the same multiprocessor. A diagram of this architecture is depicted in Figure 2, taken from Section 1.1 of NVIDIA (2012a). The scheduler on the multiprocessor then divides the user-defined blocks into smaller groups of threads that correspond to the number of cores on the multiprocessor. These smaller groups of threads are known as warps — as described in NVIDIA (2012a), “The term *warp* originates from weaving, the first parallel thread technology.” As mentioned above, each core of the multiprocessor then operates on a single thread in a warp, issuing each of the kernel instructions in parallel. This architecture is known as *Single-Instruction Multiple-Thread* (SIMT) (NVIDIA (2012a)).

Because GPUs employ SIMT architecture, it is important to avoid branch divergence among threads. While individual cores operate on individual threads, the parallel structure achieves the greatest efficiency when all cores execute the same instruction at the same time. Branching within threads is allowed, but asynchronicity may result in sequential execution over data elements of the warp. Given the specifications of GPU cores, sequential execution would be horribly inefficient relative to simply performing sequential execution on the CPU.

2.3 Software

NVIDIA was the original leader in developing a set of software tools allowing scientists to access GPUs. The CUDA C language (NVIDIA (2012a)) is simply a set of functions that can be called within basic C/C++ code that allow users to interact with GPU memory and processing cores. CUDA C is currently the most efficient and best documented way to design GPU software — it is truly the state of the art. Downsides to CUDA C are that it requires low-level comfort with software design (similar to C/C++) and that it only runs on NVIDIA GPUs running the CUDA platform. The CUDA platform itself is free, but requires NVIDIA hardware. While originally designed only for C/C++, it is now possible to write CUDA C kernels for Fortran, Python, and Java.

OpenCL (<http://www.khronos.org/opencl/>) is an open source initiative led by Apple and promoted by the Khronos Group. The syntax of OpenCL is very similar to CUDA C, but it has the advantage of not being hardware dependent. In fact, not only can OpenCL run on a variety of GPUs (including NVIDIA GPUs), it is intended to exploit the

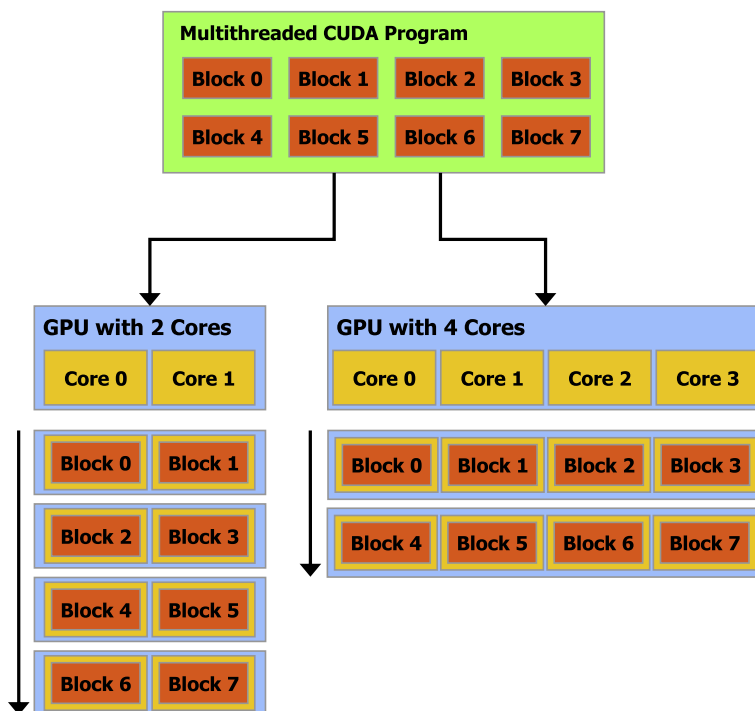


Figure 2 Schematic diagram of thread blocks and GPU multiprocessors, taken from Section 1.1 of NVIDIA (2012a). This diagram shows how (1) each thread block executes on exactly one GPU multiprocessor and (2) multiple thread blocks can be scheduled on the same multiprocessor.

heterogeneous processing resources of differing GPUs and CPUs simultaneously within one system. The downside to OpenCL is that it is poorly documented and has much less community support than CUDA C. In contrast to NVIDIA CUDA, it is currently very difficult to find a cohesive set of documentation that assists an average user in making a computer system capable of running OpenCL (e.g., downloading drivers for a GPU) and in beginning the process or software design with OpenCL.

Beyond these two foundational GPU software tools, more and more third-party vendors are developing new tools, or adding GPU functionality within current software. Examples include the Parallel Computing Toolbox in Matlab and the CUD-ALink and OpenCLLink interfaces in Mathematica. New vendors, such as AccelerEyes (<http://www.accelereyes.com/>) are developing libraries that allow higher-level interaction with the GPU: their Jacket product is supposed to be a superior parallel computing library for Matlab, and their ArrayFire product is a matrix library that allows similar high-level interaction within C, C++, and Fortran code. ArrayFire works with both the CUDA and OpenCL platforms (i.e., any GPU) and the basic version is free. For a licensing fee, users can also gain access to linear algebra and sparse grid library functions.

Similar to ArrayFire, matrix libraries such as Thrust, ViennaCL, and C++Amp have been developed to allow higher-level GPU support within the context of the C and C++ languages. All are free, although each has specific limitations: e.g., Thrust only works on the CUDA platform, and, at present, C++Amp only works on the Windows operating system via Visual Studio 2012 (and hence is not free if VS2012 cannot be obtained through an academic license). While tied to NVIDIA hardware, Thrust is a well-documented and well-supported library which will be featured below.

One of the limitations of GPU computing relative to parallel computing with traditional CPUs is that there are fewer software tools available. Further, those which are available tend to be less sophisticated. Debugging software and numerical libraries are examples—in particular, far fewer numerical libraries are currently available for GPU than CPU computing. However, given the rapid uptake of GPUs for scientific computing, this will most likely change in the near future (as evidenced by the discussion of dynamic parallelism and GPU callable libraries in [Section 6.1](#)).



3. A SIMPLE GPGPU EXAMPLE

Let us now turn to a simple problem that can be computed with a GPU and illustrate how it can be implemented in several computing languages. One of the primary objectives of this section will be to provide demonstration code that can serve as a template for using GPUs in economic research and which will serve as a foundation for understanding the applications in [Sections 4](#) and [5](#).

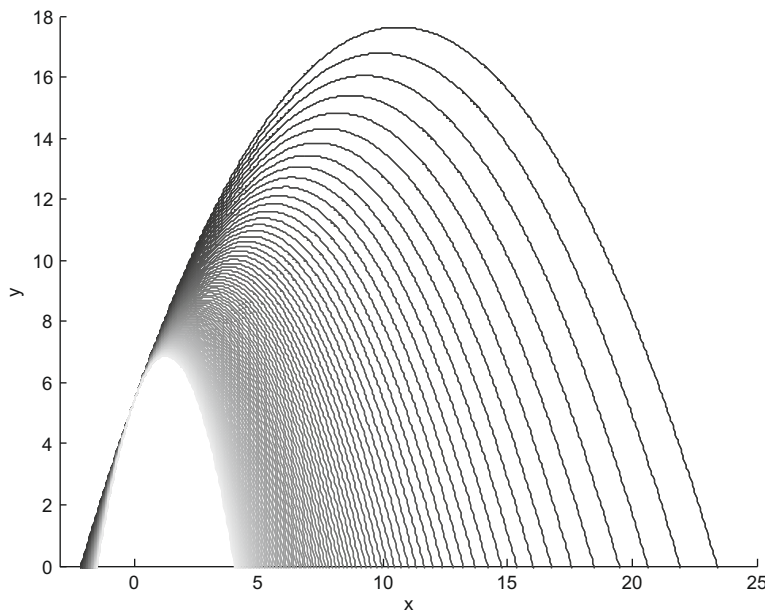


Figure 3 Second-order polynomials $ax^2 + 2.3x + 5.4$ for $a \in [-0.9, -0.1]$. The darkest line corresponds to $a = -0.1$.

Consider the second-order polynomial

$$y = ax^2 + bx + c. \quad (2)$$

Suppose that we wish to optimize the polynomial for a finite set of values of the second-order coefficient in a specific range: $a \in [-0.9, -0.1]$. **Figure 3** depicts this range of polynomials when $b = 2.3$ and $c = 5.4$, and where the darkest line corresponds to the case $a = -0.1$. In this example it is trivial to determine the location of the optimum,

$$x = -\frac{b}{2a}. \quad (3)$$

However, to illustrate the mechanics of parallel computing we will compute the solution numerically with Newton's Method for each $a \in [-0.9, -0.1]$.

The remainder of this section will show how to solve this problem with Matlab, C++, CUDA C, and Thrust.¹ The Matlab and C++ codes are provided merely as building blocks—they are not parallel implementations of the problem. In particular, the Matlab code serves as a baseline and demonstrates how to quickly solve the problem in a language that is familiar to most economists. The C++ code then demonstrates how easily the solution can be translated from Matlab to C++; indeed, most economists will be

¹ All of the code can be obtained from <http://www.parallelecon.com/basic-gpu/>.

surprised at the similarity of the two languages. Finally, understanding the serial C++ implementation is valuable for CUDA C and Thrust, since these latter implementations are simply libraries that extend the C++ framework.

3.1 Matlab

Listing 1 displays the file `main.m`, which solves the optimization problem above for various values of the second-order coefficient. The block of code on lines 2–4

```
nParam = 1000;
paramMin = -0.9;
paramMax = -0.1;
paramGrid = paramMin:((paramMax-paramMin)/(nParam-1)):paramMax;
```

constructs a grid, `paramGrid`, of `nParam = 1000` values between -0.9 and -0.1 . Line 8 then allocates a vector for storing the arg max values of the polynomial at each a ,

```
argMaxVals = zeros(nParam,1);
```

and lines 9–11 loop over each value of `paramGrid` and maximize the polynomial by calling the function `maxPoly`,

```
for i = 1:nParam
    argMaxVals(i) = maxPoly(2.2, paramGrid(i), 0.00001);
end
```

To numerically solve for the maximum at line 10, Matlab provides built-in optimization functions such as `fmincon`; alternatively, superior third-party software, such as KNITRO (<http://www.ziena.com/knitro.htm>), could be used. To keep the Matlab software similar to the implementations below, we make use of a self-written Newton solver wrapped in the function `maxPoly`, which is shown in Listing 2. The first line of the listing

Listing 1 Serial Matlab code for polynomial maximization problem: `main.m`

```
1 % Grid for order 2 coefficient
2 nParam = 1000;
3 paramMin = -0.9;
4 paramMax = -0.1;
5 paramGrid = paramMin:((paramMax-paramMin)/(nParam-1)):paramMax;
6
7 % Maximize for each coefficient
8 argMaxVals = zeros(nParam,1);
9 for i = 1:nParam
10     argMaxVals(i) = maxPoly(2.2, paramGrid(i), 0.00001);
11 end
```

```
function argMax = maxPoly(x0, coef, tol)
```

shows that `maxPoly` accepts three arguments: an initial value for x , `x0`, a value of the second-order coefficient, `coef`, and a convergence tolerance, `tol`. On exit, the function returns a single value, `argMax`, which is the arg max of the function. Lines 4 and 5

```
x = x0;  
diff = tol+1;
```

initialize the arg max, x , and create a variable, `diff`, which tracks the difference between Newton iterates of x . The main Newton step then occurs within the while loop between lines 6 and 21. In particular, lines 9 and 12 compute the first and second derivatives of the polynomial,

```
firstDeriv = 2*coef*x + 2.3;  
secondDeriv = 2*coef;
```

and line 15

Listing 2 Serial Matlab code for Newton's Method: `maxPoly.m`

```
1 function argMax = maxPoly(x0, coef, tol)  
2  
3 % Iterate to convergence  
4 x = x0;  
5 diff = tol+1;  
6 while diff > tol  
7  
8 % Compute the first derivative  
9 firstDeriv = 2*coef*x + 2.3;  
10  
11 % Compute the second derivative  
12 secondDeriv = 2*coef;  
13  
14 % Newton step  
15 xNew = x - firstDeriv/secondDeriv;  
16  
17 % Compute difference for convergence check and update  
18 diff = abs(xNew - x);  
19 x = xNew;  
20  
21 end  
22  
23 % Function output  
24 argMax = x;  
25  
26 end
```

```
xNew = x - firstDeriv/secondDeriv;
```

uses the derivatives to update the value of the arg max, `xNew`. Each iteration terminates by computing the difference between the new and current iterates

```
diff = abs(xNew - x);
```

and then setting the new value of the arg max to be the current value

```
x = xNew;
```

When convergence is achieved (`diff < tol`), the function exits and returns the most recent value of x . As is seen above, the basic nature of the problem makes it very easy to solve with few lines of code.

3.2 C++

Listings 3 and 4 display C++ code for the polynomial optimization problem. This code makes no direct advances toward parallelization, but sets the framework for subsequent parallel implementations (CUDA C and Thrust) which build on C++. While most economists are not comfortable with C++, many will be surprised by the similarity between the Matlab and C++ code, especially the functions `maxPoly.m` and `maxPoly.cpp`.

Listing 3 Serial C++ code for polynomial maximization problem: `main.cpp`

```

1 #include <Eigen/Dense>
2
3 using namespace Eigen;
4
5 double maxPoly(double x0, double coef, double tol);
6
7 int main()
8 {
9
10 // Grid for order 2 coefficient
11 int nParam = 1000;
12 double paramMin = -0.9;
13 double paramMax = -0.1;
14 VectorXd paramGrid = VectorXd::LinSpaced(nParam, paramMin, paramMax);
15
16 // Maximize for each coefficient
17 VectorXd argMaxVals = VectorXd::Zero(nParam);
18 for(int i = 0 ; i < nParam ; ++i){
19     argMaxVals(i) = maxPoly(2.2, paramGrid(i), 0.00001);
20 }
21
22 return 0;
23
24 }

```

Listing 4 Serial C++ code for Newton's Method: maxPoly.cpp

```

1 #include <math.h>
2
3 double maxPoly(double x0, double coef, double tol){
4
5     // Iterate to convergence
6     double x = x0;
7     double diff = tol+1;
8     double firstDeriv, secondDeriv, xNew;
9     while(diff > tol){
10
11         // Compute the first derivative
12         firstDeriv = 2*coef*x + 2.3;
13
14         // Compute the second derivative
15         secondDeriv = 2*coef;
16
17         // Newton step
18         xNew = x - firstDeriv/secondDeriv;
19
20         // Compute difference for convergence check and update
21         diff = fabs(xNew - x);
22         x = xNew;
23
24     }
25
26     // Function output
27     return x;
28
29 }

```

Listing 3 shows the file `main.cpp` which corresponds to the Matlab script `main.m` in Listing 1. Two general notes about C++ syntax will be beneficial:

1. Single-line comments in C++ begin with `//`, as opposed to `%` in Matlab. Multiline comments begin with `/*` and end with `*/`.
2. Functions and conditional statements in C++ begin and end with curly braces `{}`, whereas in Matlab only the end point is explicitly defined with the statement `end`.

The first notable difference between `main.cpp` and `main.m` arises in lines 1 and 3 of the former,

```

#include <Eigen/Dense>

using namespace Eigen;

```

where the Eigen library is called: Eigen (<http://eigen.tuxfamily.org>) is a template library that provides basic linear algebra functionality. By default, C++ does not load many of the basic libraries that are beneficial for scientific computing—these must be invoked explicitly in the software.

The next difference is the declaration of the function `maxPoly` in line 5

```
double maxPoly(double x0, double coef, double tol);
```

Before any variable or function can be used in C++, it must be declared and initialized. Further, declarations require a statement of type: in this case the `double` preceding the name of the function states that the function will return a double precision variable, and the instances of `double` before each of the function arguments also state that the arguments will be double precision values. The function itself is only declared in `main.cpp` and not defined—the definition is fully enclosed in `maxPoly.cpp`. However, in order to utilize the function, `main.cpp` must have access to the definition of `maxPoly` and not only its declaration. This is accomplished by linking the two C++ files at compile time, which can either be done on the command line or in a separate makefile, a topic which is beyond the scope of this paper. To see how this is accomplished in a makefile, readers can download code for this example at <http://www.parallelecon.com/basic-gpu/>.

Unlike Matlab, which allows users to write an interactive script, all C++ code must be wrapped in an outer function entitled `main`. This is seen in line 7 of Listing 3. Convention is that `main` returns an integer value: 0 if the program is successful, 1 otherwise. Within the `main` function, we see the same operations being performed as in `main.m`. First, the grid of second-order coefficients, `paramGrid`, is constructed

```
int nParam = 1000;
double paramMin = -0.9;
double paramMax = -0.1;
VectorXd paramGrid = VectorXd::LinSpaced(nParam, paramMin, paramMax);
```

Clearly, `nParam` is declared to be an integer and `paramMin` and `paramMax` are double precision. Less obviously, `paramGrid` is declared as type `VectorXd`, which is a double precision vector made available by Eigen. The function `LinSpaced(n, a, b)` constructs an equally spaced array of `n` values between `a` and `b`.

Lines 17–20

```
VectorXd argMaxVals = VectorXd::Zero(nParam);
for(int i = 0 ; i < nParam ; ++i){
    argMaxVals(i) = maxPoly(2.2, paramGrid(i), 0.00001);
}
```

then allocate storage for the arg max values and loop over `paramGrid`, performing the maximization by calling `maxPoly` for each value of the grid. Aside from previously mentioned syntactical differences, these lines are identical to their Matlab counterpart. Listings 2 and 4 show that the same is true of the functions `maxPoly.m` and `maxPoly.cpp`: aside from previously mentioned syntactical differences and line 1 of `main.cpp`

```
#include <math.h>
```

which explicitly invokes the basic math library `math.h`, these two files are essentially identical.

3.3 CUDA C

CUDA C is a set of C/C++ callable functions that provide an interface to NVIDIA graphics devices. Listings 5 and 6 display parallel GPU code, written in C++, making use of CUDA C function calls. Note that the file name extensions have been changed from `.cpp` to `.cu`. The first line of Listing 5

```
#include "maxPoly.cu"
```

Listing 5 CUDA C code for polynomial maximization problem: `main.cu`

```

1 #include <iostream>
2 #include "maxPoly.cu"
3
4 using namespace std;
5
6 int main()
7 {
8
9     // Grid for order 2 coefficient
10    int nParam = 1000;
11    double paramMin = -0.9;
12    double paramMax = -0.1;
13    double* paramGrid = new double[nParam];
14    for(int i = 0 ; i < nParam ; ++i) paramGrid[i] = paramMin + i*(paramMax-paramMin)/
        (nParam-1);
15
16    // Copy parameter grid from CPU to GPU memory
17    double* paramGridDevice;
18    cudaMalloc((void**)&paramGridDevice, nParam*sizeof(double));
19    cudaMemcpy(paramGridDevice, paramGrid, nParam*sizeof(double), cudaMemcpyHostToDevice);
20
21    // Storage for argmax values
22    double* argMaxValsDevice;
23    cudaMalloc((void**)&argMaxValsDevice, nParam*sizeof(double));
24
25    // Maximize for each coefficient
26    int threadsPerBlock = 256;
27    int blocksPerGrid = (int)ceil((double)nParam/threadsPerBlock);
28    maxPoly<<<blocksPerGrid, threadsPerBlock >>>(2.2, paramGridDevice,
29                                                0.00001, nParam, argMaxValsDevice);
30
31    // Copy argmax values from GPU to CPU memory
32    double* argMaxVals = new double[nParam];
33    cudaMemcpy(argMaxVals, argMaxValsDevice, nParam*sizeof(double), cudaMemcpyDeviceToHost);
34
35    for(int i = 0 ; i < nParam ; ++i){
36        cout << argMaxVals[i] << endl;
37    }
38
39    return 0;
40
41 }
```

Listing 6 CUDA C code for Newton's Method: maxPoly.cu

```

1 #include <math.h>
2
3 __global__ void maxPoly(double x0, double* coef,
4                       double tol, int nParam, double* argMax){
5
6     // Thread ID
7     int i = blockIdx.x*blockDim.x + threadIdx.x;
8
9     // The Kernel should only execute if i < nParam
10    if(i >= nParam){
11        return;
12    } else {
13
14        // Iterate to convergence
15        double x = x0;
16        double diff = tol+1;
17        double firstDeriv, secondDeriv, xNew;
18        while(diff > tol){
19
20            // Compute the first derivative
21            firstDeriv = 2*coef[i]*x + 2.3;
22
23            // Compute the second derivative
24            secondDeriv = 2*coef[i];
25
26            // Newton step
27            xNew = x - firstDeriv/secondDeriv;
28
29            // Compute difference for convergence check and update
30            diff = fabs(xNew - x);
31            x = xNew;
32
33        }
34
35        // Function output
36        argMax[i] = x;
37    }
38 }
39 }

```

serves the purpose of declaring and defining the function in `maxPoly.cu`. Lines 7–9 of Listing 5 show that `nParam`, `paramMin`, and `paramMax` are declared and initialized exactly as in `main.cpp`, however the initialization of `paramGrid` on lines 10 and 11 is somewhat different:

```

double* paramGrid = new double[nParam];
for(int i = 0 ; i < nParam ; ++i)
    paramGrid[i] = paramMin + i*(paramMax-paramMin)/(nParam-1);

```

Where the C++ code declared `paramGrid` to be an Eigen vector of double precision values and initialized the grid with the function `LinSpaced`, the CUDA C implementation is a bit more rudimentary: it declares a basic C array on line 10 and then initializes each value of the array with a for loop. The reason for this is that the CUDA compiler,

The `<<<x, y>>>` syntax is the core CUDA C interface to request parallel operation on a data structure. The first argument can either be an integer or a one-, two-, or three-dimensional object of type `dim3`, which specifies the dimensions of the grid containing thread blocks (i.e., the thread blocks can be arranged in an array structure of up to three dimensions). If this argument is an integer scalar N , the grid is one-dimensional with N elements (i.e., N thread blocks). The second argument is either an integer or a one- or two-dimensional object of type `dim3` which specifies the dimensions of a thread block. In the example above, `<<<blocksPerGrid, threadsPerBlock>>>` specifies a one-dimensional grid containing `blocksPerGrid = 4` one-dimensional thread blocks of `threadsPerBlock = 256` threads. Note that the syntax on line 24

```
int blocksPerGrid = (int)ceil((double)nParam/threadsPerBlock);
```

ensures that there are always enough thread blocks in the grid to contain all of the `nParam` threads by rounding the value `nParam/threadsPerBlock` up to the nearest integer (the use of `(double)` and `(int)` force all variables to be cast as the right types). The upshot is that line 25 requests the operations in the kernel `maxPoly` to be performed in parallel on blocks of 256 elements of `paramGridDevice`. It is important to note that while different block sizes are optimal for different GPUs (depending on the number of cores), this variable defines the number of threads per block and is independent of the total number of GPU cores (i.e., it does not need to be changed when moving the code from one GPU to another—even if a GPU has fewer than 256 cores).

The C++ function `maxPoly.cpp` and CUDA kernel `maxPoly.cu` are almost exactly identical. The first difference occurs in the kernel definition on line 3 of Listing 6:

```
__global__ void maxPoly(double x0, double* coef,
                        double tol, int nParam, double* argMax){
```

The following is a breakdown of the how this line differs from the corresponding definition in `maxPoly.cpp`:

- `__global__` is CUDA C syntax for declaring a kernel (referring to global device memory).
- The kernel must return type `void`, which is true of all CUDA kernels (as compared to the `double` return type of `maxPoly.cpp`). This means that `maxPoly.cu` returns nothing.
- The second argument of the kernel is the full vector (in reality, a pointer to the vector in memory) of possible second-order coefficients, rather than a single element of the coefficient array.
- The kernel has an additional argument, `nParam`, which is the integer length of the coefficient vector, `coef`.
- Because it returns `void`, the kernel has been augmented with an additional argument, `argMax`, which is an empty vector where the solutions are stored. In particular, since

a pointer to the location of the vector in memory is passed (the `*` notation) the values can be modified by the function and will remain modified upon exit.

Finally, line 6 of `maxPoly.cu`

```
int i = blockIdx.x*blockDim.x + threadIdx.x;
```

is the operative line of code that CUDA uses to assign data elements to processor threads. Within a particular kernel, the values `blockIdx.x`, `blockIdx.y`, and `blockIdx.z` correspond to the three-dimensional indices of a unique block within the grid of blocks and the values `threadIdx.x` and `threadIdx.y` are the two-dimensional indices of a unique thread within a block. Variables `blockDim.x` and `blockDim.y` correspond to the number of threads along each dimension of a block. Coupling block indices with block dimensions traverses the threads within the grid to select the initial thread element of a block within the grid. In this example, with a total of 4 blocks, `blockIdx.x` $\in \{0, 1, 2, 3\}$ (indexing in C++ begins at zero), `blockDim.x` = 256 and `threadIdx.x` $\in \{0, 1, \dots, 255\}$. Hence, the variable `i` corresponds to a unique element in the parameter grid `coef`, which is used on lines 21 and 24 and which results in a final solution, `argMax`, on line 36. The commands

```
if(i >= nParam){  
    return;  
} else {
```

on lines 10–12 ensure that the kernel only operates on array indices that are less than `nParam`. If the number of data elements is not perfectly divisible by the block size, the grid of blocks will contain thread elements which exceed the number of threads needed for computation—that is, the use of `ceil` in the code causes the number of threads in the grid of blocks to be at least as great as `nParam`. In the example above, the grid of blocks has 1024 threads, whereas the coefficient vector only has 1000 elements. Without the conditional statement above, kernels will operate on threads that exceed `nParam`, potentially altering values in memory that are reserved for computations by other multiprocessors. Hence, lines 10–12 serve as a protection for memory objects that do not belong to the coefficient vector `coef`.

In summary, this code allows the CUDA runtime environment to divide thread blocks among available multiprocessors, which then schedules individual threads to individual cores. As emphasized above, the scheduling of blocks is transparent to the user and scales automatically to the number of multiprocessors. Each thread process then accesses a unique ID in the thread block via the `threadIdx` command. The end result is that the sequential loop is eliminated and each GPU core is able to issue the kernel instructions for optimization in parallel on individual elements of the parameter vector. Because of transparent scaling, this code can run on a laptop with only 32 GPU cores or on a Tesla C2075 with 448 cores without modification.

3.4 Thrust

As mentioned above, Thrust is a free template library that can be called within C/C++ and which provides an alternate interface to GPU hardware. Listings 7 and 8 display parallel GPU code written in C++, making use of the Thrust template library. The primary advantage of Thrust is that it combines the conciseness of Matlab and C++/Eigen code with the ability to schedule parallel work on a GPU. In particular, Thrust eliminates the need for explicit memory allocation and transfer between host and device. Although the transfer *must still occur*, allocating and copying a data object in device memory is as simple as

```
double* Y = new double[N]; // Allocate a vector, Y, of N elements in
host memory

thrust::device_vector<double> X = Y; // Allocate and copy to device memory
```

in contrast to the excessively verbose use of `cudaMalloc` and `cudaMemcpy` in CUDAC. This greatly facilitates the development of software as it allows the user to work at a high level of abstraction, without the need to deal with the minor details of memory allocation and transfer.

Lines 1–3 of Listing 7 include the relevant Thrust libraries for use in C++ and line 4

Listing 7 Thrust code for polynomial maximization problem: main.cu

```
1 #include <iostream>
2 #include <thrust/device_vector.h>
3 #include <thrust/sequence.h>
4 #include <thrust/transform.h>
5 #include "maxPoly.hpp"
6
7 using namespace std;
8
9 int main()
10 {
11
12     // Grid for order 2 coefficient
13     int nParam = 1000;
14     double paramMin = -0.9;
15     double paramMax = -0.1;
16     thrust::device_vector<double> paramGrid(nParam);
17     thrust::sequence(paramGrid.begin(), paramGrid.end(), paramMin, (paramMax-paramMin)/
18         (nParam-1));
19
20     // Maximize for each coefficient
21     thrust::device_vector<double> argMaxVals(nParam);
22     thrust::transform(paramGrid.begin(), paramGrid.end(), argMaxVals.begin(), maxPoly(2.2,
23         0.00001));
24
25     for(int i = 0 ; i < nParam ; ++i){
26         cout << argMaxVals[i] << endl;
27     }
28
29     return 0;
30 }
```

Listing 8 Thrust code for Newton's Method: maxPoly.hpp

```

1 #include <math.h>
2
3 struct maxPoly{
4
5     // Arguments
6     const double x0; ///< Initial value
7     const double tol; ///< Convergence criterion
8
9     /// Constructor
10    maxPoly(const double _x0, const double _tol) : x0(_x0), tol(_tol) {}
11
12    /// Kernel
13    __host__ __device__
14    double operator()(const double coef) const {
15
16        // Iterate to convergence
17        double x = x0;
18        double diff = tol+1;
19        double firstDeriv, secondDeriv, xNew;
20        while(diff > tol){
21
22            // Compute the first derivative
23            firstDeriv = 2*coef*x + 2.3;
24
25            // Compute the second derivative
26            secondDeriv = 2*coef;
27
28            // Newton step
29            xNew = x - firstDeriv/secondDeriv;
30
31            // Compute difference for convergence check and update
32            diff = fabs(xNew - x);
33            x = xNew;
34        }
35
36        // Function output
37        return x;
38    }
39 }
40 };
41
42 };

```

```
#include "maxPoly.hpp"
```

is the equivalent of including the maxPoly kernel source code, which will be described below. The declarations of nParam, paramMin, and paramMax on lines 10–12 are identical to those in C++ and CUDA C, so the first major difference arises on lines 13 and 14 with the declaration and initialization of paramGrid:

```

thrust::device_vector<double> paramGrid(nParam);
thrust::sequence(paramGrid.begin(), paramGrid.end(),
                paramMin, (paramMax-paramMin)/(nParam-1));

```

The syntax `thrust::device_vector` instantiates a vector directly in device memory. The function `thrust::sequence(start, end, lower, step)` then constructs an equally spaced sequence of points between the positions `start` and `end`

of a Thrust vector, beginning at the value `lower`, with the grid points `step` units apart. Unlike CUDA C, where `paramGrid` first had to be computed in host memory and transferred to device memory, we see that Thrust allows functionality to build such a grid directly in the device memory. This not only saves time in transferring data, but also results in more streamlined code.

Line 17 then declares and allocates memory for a device vector, `argMaxVals`, which is not transferred to host memory at the end of the program because Thrust allows users to access and manipulate members of a device vector as if they reside in host memory. The important parallel operation of the file occurs at line 18:

```
thrust::transform(paramGrid.begin(), paramGrid.end(),
                 argMaxVals.begin(), maxPoly(2.2, 0.00001));
```

In contrast to the `<<<x,y>>>` syntax of CUDA C, the parallel interface in Thrust is provided by two functions: `thrust::transform` and `thrust::for_each`. Specifically,

```
thrust::transform(inputStart, inputEnd, outputStart, function)
```

applies `function` to each element of a Thrust vector between `inputStart` and `inputEnd` and places the output in the Thrust vector starting at `outputStart`. Although it is not described here, `thrust::for_each` provides similar functionality. Most users find this interface to be a bit more intuitive than that of CUDA C.

While we previously saw that the files `maxPoly.m`, `maxPoly.cpp`, and `maxPoly.cu` were almost identical, a brief glance at Listing 8 shows substantial differences in the Thrust equivalent, `maxPoly.hpp` (which is referred to as a “functor” or function object). The major differences arise from the fact that Thrust encloses the “kernel” in a C++ class structure rather than in a simple function. Line 3

```
struct maxPoly{
```

is the C/C++ syntax for declaring such an object and Lines 6, 7, and 10

```
const double x0; ///< Initial value
const double tol; ///< Convergence criterion
maxPoly(const double _x0, const double _tol) : x0(_x0), tol(_tol) {}
```

declare the members of the object. In this case, the members are the actual function `maxPoly` and the arguments to the function (the initial value of the arg max, `x0`, and the Newton convergence tolerance, `tol`). Lines 13 and 14

```
__host__ __device__
```

```
double operator()(const double coef) const {
```

provide the syntax for an operator `()`, which is the object interface for `maxPoly`, and the instructions between lines 14 and 35 are identical to those found in `maxPoly.cpp`.

Note that there is no explicit use of a thread ID in Thrust, nor does `maxPoly` take `paramGrid` as an argument—these details are handled transparently via `thrust::transform`. Also, where users must specify a thread block structure in CUDA C, Thrust handles details of blocks and grids under the hood.

The final advantage of Thrust is that it has separate backends for CUDA and OpenMP; that is, the same software can access GPU or shared-memory CPU parallelism (although not both at the same time). The result is that Thrust software can run without modification on systems that do not have GPU capabilities, but that have multiple CPUs cores that share memory. This will be demonstrated in the examples of the following sections. For more details on using the Thrust interface, see [Bell and Hoberock \(2012\)](#) or the Thrust Quickstart Guide ([NVIDIA \(2012b\)](#)).



4. EXAMPLE: VALUE FUNCTION ITERATION

We will now turn our attention to a specific example where parallelism can greatly speed up the computation of an economic model. Specifically, we will consider a canonical real business cycle (RBC) model ([Kydland and Prescott \(1982\)](#)) solved with value function iteration (VFI) ([Judd \(1998\)](#)). While this model is simple, it is an excellent illustration of the benefits of a parallel architecture. The results of this section are based upon those of [Aldrich et al. \(2011\)](#) with some minor modifications and code to replicate the results is available at <http://www.parallelecon.com/vfi/>.

4.1 Model

The economy is populated by a representative agent with preferences over a single consumption good. The agent seeks to maximize expected lifetime utility,

$$\mathbb{E}_0 \left[\sum_{t=0}^{\infty} \beta^t u(C_t) \right], \quad (4)$$

where C_t is the agent's consumption at time t , \mathbb{E}_0 is the conditional expectations operator at $t = 0$, and β is the discount factor. For this example we specialize the period utility function to be of the constant relative risk aversion form:

$$u(C_t) = \frac{C_t^{1-\gamma}}{1-\gamma}, \quad (5)$$

where γ is the coefficient of relative risk aversion.

The agent receives income each period by renting labor and capital to a representative firm and chooses consumption and investment so as to satisfy the budget constraints

$$C_t + I_t = w_t + r_t K_t, \quad \forall t, \quad (6)$$

where w_t is the wage paid for a unit of labor, r_t is the rental rate for a unit of capital, K_t is capital, I_t is investment, and where we have assumed that labor, L_t , is normalized to unity and supplied inelastically because it does not enter the agent's utility function. Capital depreciates each period according to

$$K_{t+1} = I_t + (1 - \delta)K_t, \quad \forall t, \quad (7)$$

where δ is the depreciation rate.

The representative firm produces output according to

$$Y_t = Z_t f(K_t), \quad \forall t \quad (8)$$

where Y_t is output and where the total factor of productivity (TFP), Z_t , follows the law of motion

$$\log(Z_t) = \rho \log(Z_{t-1}) + \varepsilon_t, \quad \text{where } \varepsilon_t \stackrel{i.i.d.}{\sim} \mathcal{N}(0, \sigma^2), \quad \forall t, \quad (9)$$

We will assume that the production function is of the Cobb-Douglas form:

$$f(K_t) = K_t^\alpha, \quad (10)$$

where α is the output elasticity of capital. Combining Eqs. (6)–(8) with the market clearing condition $C_t = Y_t$, we arrive at the aggregate resource constraint

$$K_{t+1} + C_t = Z_t K_t^\alpha + (1 - \delta)K_t, \quad \forall t. \quad (11)$$

Since the welfare theorems are satisfied, we can find the agent's optimal consumption path by solving a recursive version of a social planner's problem

$$V(K, Z) = \max_c \left\{ \frac{C^{1-\gamma}}{1-\gamma} + \beta \mathbb{E} [V(K', Z') \mid Z] \right\} \quad (12a)$$

subject to

$$K' = ZK^\alpha + (1 - \delta)K - C \quad (12b)$$

$$\log(Z') = \rho \log(Z) + \varepsilon', \quad \varepsilon' \sim \mathcal{N}(0, \sigma^2), \quad (12c)$$

where the recursive structure of the problem allows us to simplify notation by dropping time subscripts: a variable X refers to its value in the current time period, while X' denotes its value in the subsequent period. It is not requisite to solve the model with VFI in order to achieve the advantages of massive parallelism—we could obtain similar benefits by working directly with the equilibrium conditions. However, the problem is most easily illustrated in the present format.

4.2 Solution

Since $\beta \in (0, 1)$, $\delta \in (0, 1)$, $u(C)$ and $f(K)$ are both continuous, strictly increasing and concave, and ε_t are i.i.d. shocks drawn according to a Lebesgue probability measure, Theorem 9.8 of [Stokey et al. \(1989\)](#) proves that System (12) has a unique functional solution $V(\cdot, \cdot)$ and that there also exists a unique policy function, G , for the endogenous state variable, $K : K' = G(K, Z)$. Unfortunately, there are no closed-form, analytical solutions for V and G , so they must be approximated numerically. [Judd \(1998\)](#) highlights several ways to arrive at numerical solutions for this problem, one of which is value function iteration (VFI). In brief, VFI specifies a domain $(K, Z) \in [\underline{K}, \overline{K}] \times [\underline{Z}, \overline{Z}]$ and a functional form for V . Discretizing the domain and starting with an initial guess, V^0 , for the value function, VFI iterates on System (12), using a numerical integration method, until successive iterates of the value function converge. Convergence for this problem is guaranteed by Theorem 9.6 of [Stokey et al. \(1989\)](#).

Given discretizations \mathcal{K} and \mathcal{Z} of $[\underline{K}, \overline{K}]$ and $[\underline{Z}, \overline{Z}]$, a sequential implementation of VFI would use the current iterate of the value function, $V^{(i)}$, to iterate through pairs of points in $\mathcal{K} \times \mathcal{Z}$ and solve the optimization problem of System (12). The result would be an updated value function, $V^{(i+1)}$, computed in a serial fashion over each pair of state values. The algorithm would then repeat the procedure until convergence of the value function. [Algorithm 1](#) writes the VFI computations explicitly. In summary, a serial implementation loops through the grid values in Steps 6 and 7 in sequence, performing the maximization in [Eq. \(13\)](#) for each pair. Note that if either \mathcal{K} or \mathcal{Z} is a very dense grid, Step 8 may involve many thousands of serial calculations for each of the values in the loops at Steps 6 and 7.

Alternatively, with many processing cores available, the maximization problems computed for each (K, Z) pair could be assigned to individual cores and computed in parallel. In [Algorithm 1](#) this amounts to eliminating the loops in Steps 6 and 7 and outsourcing the computations of [Eq. \(13\)](#) to multiple cores. The reason that parallelism can be exploited in this problem is that the maximization nested within Steps 6 and 7 depends only on the concurrent (K, Z) and not on other values in \mathcal{K} and \mathcal{Z} . [Aldrich et al. \(2011\)](#) implement this algorithm and [Section 4.3](#) reports updated results from that paper.

As a final note, the maximization in [Eq. \(13\)](#) can be performed in a variety of ways. The results below make use of a simple binary search procedure which iteratively bisects \mathcal{K} until an optimal value of K' is found (see p. 26 of [Heer and Maussner \(2005\)](#) for an explicit algorithm). This algorithm is quite efficient, arriving at a solution in no more than $\log_2(N_k)$ steps, where N_k is the number of elements in \mathcal{K} .

4.3 Results

[Table 1](#) reports calibrated parameter values for the model. These values are standard in the literature for a quarterly calibration of a basic RBC model.

Algorithm 1. Value Function Iteration for RBC Model

- 1: Fix some $\tau > 0$ which will determine convergence and set $\varepsilon = \tau + 1$.
- 2: Compute the deterministic steady-state level of capital, K_{ss} , and set $\underline{K} = 0.95K_{ss}$ and $\bar{K} = 1.05K_{ss}$. Discretize the state space for capital so that it is confined to a grid of N_k equally spaced values between \underline{K} and \bar{K} . Denote the grid by \mathcal{K} .
- 3: Use the method of [Tauchen \(1986\)](#) to discretize the state space for the log of TFP so that it is confined to a grid of N_z equally spaced values between \underline{z} and \bar{z} (where $z = \log(Z)$). Denote the grid for TFP levels by \mathcal{Z} and the matrix of transition probabilities P , where the probability of transitioning from Z to Z' is expressed as $P(Z, Z')$.
- 4: Guess initial values of the value function, V^0 , for each pair of possible values of the state variables, K and Z (i.e., V^0 is an $N_k \times N_z$ matrix). In particular, set V^0 to be equal to the deterministic steady-state values of the value function.
- 5: **while** $\varepsilon > \tau$ **do**
- 6: **for** each $K \in \mathcal{K}$ **do**
- 7: **for** each $Z \in \mathcal{Z}$ **do**
- 8: Solve

$$\max_{K' \in \mathcal{K}} \left\{ \frac{C(K, Z, K')^{1-\gamma}}{1-\gamma} + \text{Exp}(K, Z, K') \right\}. \quad (13)$$

where

$$C(K, Z, K') = ZK^\alpha + (1 - \delta)K - K' \quad (14)$$

$$\text{Exp}(K, Z, K') = \sum_{Z' \in \mathcal{Z}} V^0(K', Z') * P(Z, Z') \quad (15)$$

- 9: **end for**
- 10: **end for**
- 11: Compute the difference between the updated value function and V^0 :

$$\varepsilon = \| V - V^0 \|_\infty. \quad (16)$$

- 12: Set $V^0 = V$.
- 13: **end while**

Table 1 Model calibration.

β	γ	α	δ	ρ	σ
0.984	2	0.35	0.01	0.95	0.005

All solutions were computed in double precision with a convergence criterion of $\tau = (1 - \beta)1e - 8$. The grid for TFP was discretized over four values using the method of [Tauchen \(1986\)](#). The grid for capital was discretized with increasing density in order to assess the performance of GPU parallelism as the solution becomes increasingly precise.

Table 2 Timing results (in seconds) for the RBC/VFI problem. “Serial CPP” and “Serial Matlab” refer to the serial implementations of the algorithm in C++ (using the Eigen library) and Matlab. “Thrust/OpenMP” and “Thrust/CUDA” refer to the Thrust implementation, using the separate backends for OpenMP (on the Quad-Core Xeon CPU) and CUDA (on the Tesla C2075).

N_k	128	256	512	1,024	2,048	4,096	8,192	16,384	32,768	65,536
Serial CPP	0.7894	2.009	5.377	16.53	56.64	202.35	869.67	3621.39	14711	58754
Serial Matlab	44.39	91.12	189.59	410.36	938.84	2722.74	9743.7	36169	139270	546360
Thrust/OpenMP (1-core)	0.4875	1.058	2.286	4.925	10.69	22.56	48.05	102.40	217.45	464.80
Thrust/OpenMP (4-core)	0.1486	0.6552	0.6992	1.375	3.008	6.396	13.59	29.45	60.41	127.91
Thrust/CUDA	6.940	6.929	6.937	6.991	7.318	7.784	8.761	10.83	15.18	23.88

Table 2 reports timing results for various software implementations of Algorithm 1. The methods include

- Single-threaded, sequential C++, making use of the Eigen template library for linear algebra computations.
- Single-threaded, sequential Matlab. This is done to compare with what the majority of economists would use to solve the problem.
- Thrust, using the OpenMP backend to solve the problem on a single core and in parallel on four CPU cores.
- Thrust, using the CUDA backend to solve the problem in parallel on the GPU.

All results were obtained on a 4U rackmount server with a single quad-core Intel Xeon 2.4 GHz CPU and two NVIDIA Tesla C2075 GPUs, although only one of the GPUs was used for the Thrust/CUDA and CUDA C timing results. The Thrust/OpenMP software, however, made use of all four of the CPU cores.

Table 2 demonstrates the great benefits of parallelism for the VFI problem. Most notably, as the capital grid density increases, the GPU implementation becomes increasingly fast relative to the serial C++ and Matlab times, where at the largest grid size considered ($N_k = 65,536$) Thrust/CUDA times are roughly 2,500 and 23,000 times faster, respectively. Not only does this show the gains from GPU parallelism, but it also highlights the speed gains in moving from Matlab to a serial C++ implementation. It is also noteworthy that the GPU implementation has an overhead cost for initializing the CUDA runtime environment which corresponds to just <7 s. This overhead cost swamps the computation times for small grid sizes and results in the GPU only improving upon the serial C++ solution for $N_k \geq 1024$. It should also be noted that the serial C++ code could be further improved by employing optimizations suggested by Lee et al. (2010b)—the code used for this problem was similar in structure to the Matlab implementation and employed only standard default optimizations with the C++ compiler (gcc 4.4.7).

A rather surprising result is the performance of Thrust/OpenMP on a single-core. Table 2 shows that the single-core Thrust solution is up to 125 times faster than the

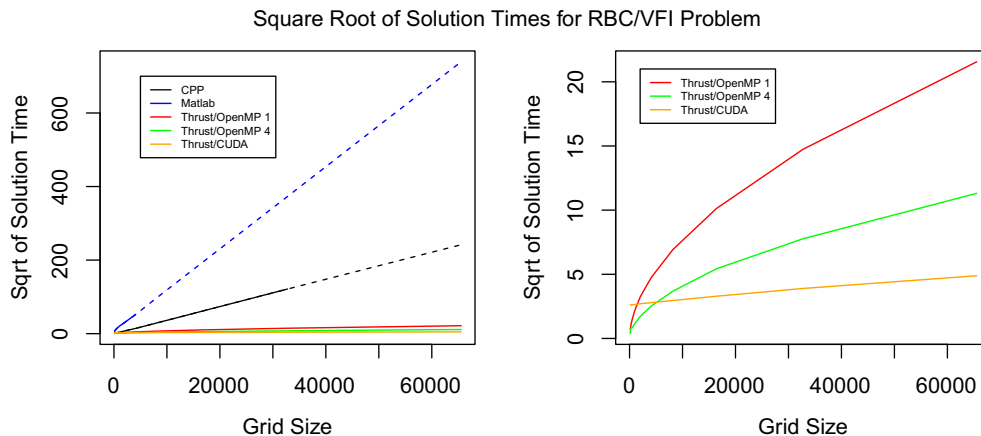


Figure 4 Square root of solution times for serial CPP (black), serial Matlab (blue), single-core Thrust/OpenMP (red), quad-core Thrust/OpenMP (green), and Thrust/CUDA (orange). (For interpretation of the references to color in this figure legend, the reader is referred to the web version of this book.)

single-core C++/Eigen solution, when $N_k = 65,536$. This improvement may be a result of CPU optimizations mentioned above. As expected, the quad-core Thrust/OpenMP solution is almost uniformly 3.5–3.6 times faster than the single-core Thrust solution for $N_k \geq 1024$ (corresponding roughly to four times the number of cores net some OpenMP overhead cost and the fraction of the program that must be run sequentially).

Overall, comparing each of the Thrust solutions that make use of all GPU cores (Thrust/CUDA) and all CPU cores (quad-core Thrust/OpenMP), we see a maximum speedup of a little more than five times for the GPU. Figure 4 depicts the square root of solution times for each of the solution methods reported in Table 2, as a function of N_k . The left panel shows all methods and the right panel excludes serial C++ and Matlab in order to better visualize the remaining methods.

When comparing the solution times, it is important to remember that CPUs and GPUs cost different amounts of money. The Tesla C2075 GPU and the quad-core Xeon CPU used in this section cost \$2120.79 and \$339.03, respectively. This means that one could purchase roughly $2120.79/339.03 \approx 6.25$ quad-core 2.4 GHz Xeon processors for the same amount of money as a single Tesla C2075 GPU. Figure 5 scales all of the computation times by processor cost, resulting in time \times dollar units. For single-core solutions (serial C++, serial Matlab, and Thrust/OpenMP single-core) the times are scaled by 1/4 the price of the Xeon CPU.

When accounting for cost, the Thrust/OpenMP methods have a slight advantage over the Thrust/CUDA method, with the scaled times approaching each other as N_k rises. This scaling suggests a slight advantage to purchasing several CPUs rather than one GPU,

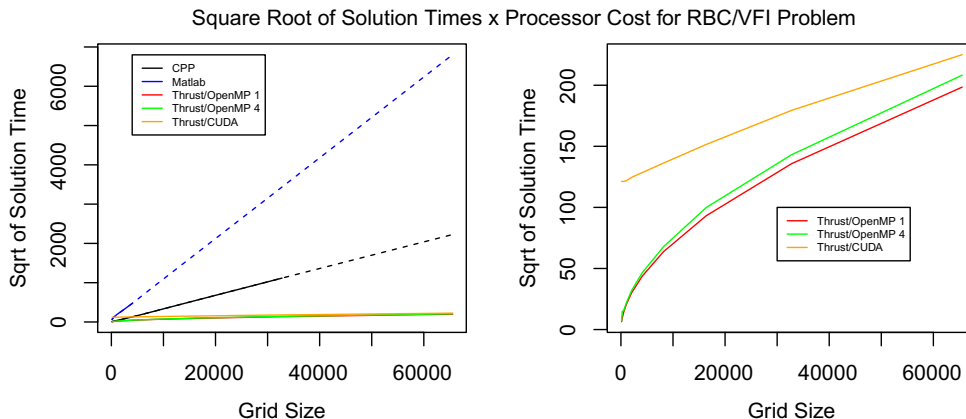


Figure 5 Square root of solution times multiplied by processor cost for serial CPP (black), serial Matlab (blue), single-core Thrust/OpenMP (red), quad-core Thrust/OpenMP (green), and Thrust/CUDA (orange). The single cores solution times (serial C++, serial Matlab, and Thrust/OpenMP single-core) are scaled by 1/4 the cost of the Xeon CPU. (For interpretation of the references to color in this figure legend, the reader is referred to the web version of this book.)

so long as one uses the Thrust library. However, this assumption does not account for the fact that the Thrust software would not automatically scale across several distinct CPUs—care would have to be taken to rewrite portions of the software to include message passing across devices. Alternatively, purchasing a single CPU with more cores (so that explicit message passing is not required in the Thrust implementation) would drive up the per-core price of the CPU and erode its economic advantage over the GPU. One final consideration is important in this context: several new GPUs are already available which would likely achieve different results for the VFI problem. Two examples are the NVIDIA GeForce GTX Titan and the NVIDIA Kepler K20. The Titan has 2688 cores and costs on the order of \$1000 while the K20 has 2496 cores and costs roughly \$3200. The low per-core cost of the Titan is due to the fact that it is a consumer-grade GPU which is optimized for single-precision operations (although it is capable of double precision). Relative to the Tesla C2075 with 448 cores, both the Titan and K20 have a much lower per-core cost.

5. EXAMPLE: A GENERAL EQUILIBRIUM ASSET PRICING MODEL WITH HETEROGENEOUS BELIEFS

Aldrich (2011) investigates asset exchange within a general equilibrium model with heterogeneous beliefs about the evolution of aggregate uncertainty. This section will outline the model and solution method of that paper and report the computational

benefits of GPU parallelism. The economic implications of the model are not treated here. See Aldrich (2011) for a complete discussion.

5.1 Model

The primary objective of the model in Aldrich (2011) is to understand the role of belief heterogeneity in generating trading volume, relative to other forms of agent heterogeneity. The paper demonstrates how small perturbations in agent beliefs can generate empirically plausible levels of trading volume within an economy that is calibrated to broadly replicate macroeconomic consumption dynamics. In order to highlight only the trading effects of belief heterogeneity, the structure of the model is very basic.

We consider a simple endowment economy with I types of agents and S aggregate states of nature each period. Time is discrete and indexed by $t \in \mathcal{N}_0 = \{0, 1, 2, \dots\}$. The aggregate state at time t is $s_t \in \mathcal{S} = \{1, \dots, S\}$ and we let $s^t = (s_0, s_1, \dots, s_t)$ denote the history of aggregate states. Agents' types are indexed by $i \in \mathcal{I} = \{1, 2, \dots, I\}$ and $\mu^i(s^t)$ denotes the proportion of the population consisting of type i agents in state s^t . The total population has unit mass, which dictates $\sum_{i=1}^I \mu^i(s^t) = 1$, for all $s^t \in \mathcal{S}^t$.

There is a single consumption good and a tree paying a dividend of $d(s^t)$ units of the consumption good in each state $s^t \in \mathcal{S}^t$, which cannot be transferred between time periods. By default, each agent is entitled to $d(s^t)$ units of consumption in state s^t , resulting in an endowment of $\mu^i(s^t)d(s^t)$ for cohort i and an aggregate endowment of $\sum_{i=1}^I \mu^i(s^t)d(s^t) = d(s^t)$. Agents have preferences for consumption encapsulated in period utility $u_i(c)$, which is type specific and which satisfies the usual conditions of strict monotonicity, strict concavity, twice continuous differentiability, and $\lim_{c \rightarrow 0} u'_i(c) = \infty$.

The aggregate state follows an S -state Markov process: the probability of history s^t is $\pi(s^t) = \pi(s_t | s_{t-1}) \cdots \pi(s_1 | s_0)\pi(s_0)$, where $s_0 \in \mathcal{S}$ is known and hence $\pi(s_0) = 1$. Aside from preference and endowment heterogeneity, encapsulated in $u_i(c)$ and $\mu^i(s^t)d(s^t)$, respectively, we allow agent types to have heterogeneous discount factors, β_i , and heterogeneous beliefs about transition probabilities, $\pi^i(s^t) = \pi^i(s_t | s_{t-1}) \cdots \pi^i(s_1 | s_0)$.

Markets are complete and agent types can deviate from their endowments by purchasing state-contingent consumption, $c^i(s^t)$. As discussed below, the results of the paper are unchanged for general asset markets, allowing agents access to assets with varying maturities and payoff structures, so long as markets are complete. The results, however, are easiest to understand within the framework of state-contingent consumption purchases. We denote the time zero price of consumption in state s^t as $q^0(s^t)$. The resulting optimization problem for an individual agent of type i is

$$U_i(c^i) = \max_{c^i} \left\{ u(c^i(s_0)) + \sum_{t=1}^{\infty} \beta_i^t \sum_{s^t} u_i(c^i(s^t)) \pi^i(s^t) \right\} \quad (17a)$$

subject to

$$c^i(s_0) + \sum_{t=1}^{\infty} \sum_{s^t} q^0(s^t) c^i(s^t) \leq d(s_0) + \sum_{t=1}^T \sum_{s^t} q^0(s^t) d(s^t), \quad (17b)$$

where $\mathbf{c}^i = (c(s_0), c(s^1), \dots)$ and where $q^0(s_0) = 1$.

A competitive equilibrium for this economy is a collection of consumption plans $\{\bar{c}^i\}_{i=1}^I$ and prices $\{\{q^0(s^t)\}_{s^t \in \mathcal{S}^t}\}_{t=0}^{\infty}$ such that

1. System (17) is solved.
2. The aggregate resource constraint

$$\sum_{i=1}^I \mu^i(s^t) \bar{c}^i(s^t) = \sum_{i=1}^I \mu^i(s^t) d(s^t) \quad (18)$$

holds for all $s^t \in \mathcal{S}^t$ and $t \geq 0$.

5.1.1 First-Order Conditions

The first-order conditions of System (17) are

$$u'_i(c^i(s_0)) = \lambda^i \quad (19a)$$

$$\beta_i^t u'_i(c^i(s^t)) \pi^i(s^t) = \lambda^i q^0(s^t), \forall s^t \in \mathcal{S}^t \quad (19b)$$

$$d(s_0) + \sum_{t=1}^T \sum_{s^t} q^0(s^t) d(s^t) - c^i(s_0) - \sum_{t=1}^T \sum_{s^t} q^0(s^t) c^i(s^t) = 0 \quad (19c)$$

for $i = 1, \dots, I$, where λ^i is agent i 's Lagrange multiplier for constraint (17b). The intertemporal Euler equation is obtained by dividing (19b) by (19a),

$$\beta_i^t \frac{u'_i(c^i(s^t))}{u'_i(c^i(s_0))} \pi^i(s^t) = q^0(s^t), \quad (20)$$

for all $s^t \in \mathcal{S}^t$ and $i = 1, \dots, I$. Selecting agent 1 as a “reference” agent, Eq. (20) yields

$$\frac{\beta_i^t u'_i(c^i(s^t))/u'_i(c^i(s_0)) \pi^i(s^t)}{\beta_1^t u'_1(c^1(s^t))/u'_1(c^1(s_0)) \pi^1(s^t)} = 1. \quad (21)$$

Reformulating (21), we arrive at

$$c^i(s^t) = u_i^{-1} \left(\frac{\beta_1^t \pi^1(s^t) u'_1(c^1(s^t))}{\beta_i^t \pi^i(s^t) u'_1(c^1(s_0))} u'_i(c^i(s_0)) \right). \quad (22)$$

Substituting Eq. (22) into the aggregate resource constraint (18),

$$\sum_{i=1}^I \mu^i(s^t) u_i^{-1} \left(\frac{\beta_1^t \pi^1(s^t) u'_1(c^1(s^t))}{\beta_i^t \pi^i(s^t) u'_1(c^1(s_0))} u'_i(c^i(s_0)) \right) = \sum_{i=1}^I \mu^i(s^t) d(s^t). \quad (23)$$

For each $s^t \in \mathcal{S}^t$ and $t \geq 0$, given discount rates, $\{\beta_i\}_{i=1}^I$, beliefs, $\{\pi^i(s^t)\}_{i=1}^I$, period utilities, $\{u_i(c)\}_{i=1}^I$, population proportions, $\{\mu^i(s^t)\}_{i=1}^I$, and initial consumption choices, $\{c^i(s_0)\}_{i=1}^I$, Eq. (23) represents a single nonlinear equation with a single unknown, $c^1(s^t)$. If $c^i(s_0) = \bar{c}^i(s_0)$ for $i = 1, \dots, I$, the optimal initial consumption values in competitive equilibrium, the values of $c^1(s^t)$ and $\{c^i(s^t)\}_{i=2}^I$ which solve Eqs. (23) and (22), respectively, will also be the optimal competitive equilibrium values, $\bar{c}^1(s^t)$ and $\{\bar{c}^i(s^t)\}_{i=2}^I$, for all $s^t \in \mathcal{S}^t$ and $t \geq 0$. In the general formulation, these optimal choices are history dependent.

5.2 Solution

Solving a finite horizon version of this model can become computationally challenging as the time horizon, T , grows large. To solve the model, one would posit values for $\{\bar{c}^i(s_0)\}_{i=1}^I$ and then solve Eqs. (23) and (22) for $\{\bar{c}^i(s^t)\}_{i=1}^I$ at each possible state of the world s^t prior to T . The full sequence of optimal consumption values for all agents could then be substituted into the aggregate resource constraint

$$\sum_{i=1}^I \mu^i(s^t) \bar{c}^i(s^t) = \sum_{i=1}^I \mu^i(s^t) d(s^t), \quad (18)$$

to determine the quality of the initial guess for $\{\bar{c}^i(s_0)\}_{i=1}^I$. If the constraint does not hold, an informed update could be made for the initial consumption values and the entire procedure could be repeated to convergence.

A serial implementation of the solution would involve an outer loop that forms a candidate solution of optimal consumption values based on a guess for $\{\bar{c}^i(s_0)\}_{i=1}^I$, and would use the resource constraint in Eq. (18) to iteratively update those values until convergence is achieved. Within the outer loop, a single processing core would then move sequentially through each state s^t , $t \leq T$, solving the nonlinear Eq. (23) for $\bar{c}^1(s^t)$ and subsequently determining $\{\bar{c}^i(s^t)\}_{i=2}^I$ with Eq. (22), conditional on the values $\{\bar{c}^i(s_0)\}_{i=1}^I$. Algorithm 2 formally outlines these computations: line 3 represents the outer iterative loop, and Eq. (24) represents that nonlinear equation that must be solved at each node in the loops at lines 4 and 5.

For a $T + 1$ -period economy, there are a total of $\frac{S^{T+1}-1}{S-1}$ states: S^t at each time period $t = 0, 1, \dots, T$. Clearly, as T grows, the total number of states, and hence systems of nonlinear equations to solve, grows exponentially, which eventually becomes infeasible for a serial processing implementation. Figure 6 depicts an example with $S = 2$ and $T = 3$. When $T = 20$ this would translate into more than two million nonlinear equations to be solved serially within each of the outer loops of the algorithm.

It is important to note that Eqs. (23) and (22) determine a solution for $\{c^i(s^t)\}_{i=1}^I$ at each of the $\frac{S^{T+1}-1}{S-1} - 1$ states after $t = 0$, independent of the consumption choices at other dates and states in the economy. This independence between states allows the computation to be divided into distinct pieces, each of which can be performed by a

separate processing core. For [Algorithm 2](#), this amounts to outsourcing the work of lines 4–11 to individual cores. In theory, with enough cores, it would be possible to assign the nonlinear equation problem ([Eq. \(23\)](#)) of each state to one core. In practice, with large S or large T , a subset of state-tree nodes would be assigned to each core for computation. In fact, when S and T are large, this problem is ideally suited for GPU computing (as shown in the following section).

Algorithm 2. Solution of General Equilibrium Model with Heterogeneous Beliefs

- 1: Fix some $\tau > 0$, which will determine convergence and set $\varepsilon = \tau + 1$.
- 2: Guess initial values for $c^i(s_0), i = 2, \dots, N$.
- 3: **while** $\varepsilon > \tau$ **do**
- 4: **for** $t = 1, \dots, T$ **do**
- 5: **for** $s^t \in \mathcal{S}^t$ **do**
- 6: Determine $c^1(s^t)$ such that

$$\sum_{i=1}^I \mu^i(s^t) u_i'^{-1} \left(\frac{\beta_1^i \pi^1(s^t) u_1'(c^1(s^t))}{\beta_i^i \pi^i(s^t) u_1'(c^1(s_0))} u_i'(c^i(s_0)) \right) = \sum_{i=1}^I \mu^i(s^t) d(s^t). \quad (24)$$

- 7: **for** $i = 2, \dots, I$ **do**
- 8: Compute

$$q^0(s^t) = \beta_1^t \frac{u_1'(c^1(s^t))}{u_1'(c^1(s_0))} \pi^1(s^t) \quad (25)$$

$$c^i(s^t) = u_i'^{-1} \left(\frac{\beta_1^t \pi^1(s^t) u_1'(c^1(s^t))}{\beta_i^t \pi^i(s^t) u_1'(c^1(s_0))} u_i'(c^i(s_0)) \right). \quad (26)$$

- 9: **end for**
- 10: **end for**
- 11: **end for**
- 12: **for** $i = 2, \dots, N$ **do**
- 13: Compute

$$\varepsilon^i = d(s_0) + \sum_{t=1}^T \sum_{s^t} q^0(s^t) d(s^t) - c^i(s_0) - \sum_{t=1}^T \sum_{s^t} q^0(s^t) c^i(s^t). \quad (27)$$

- 14: **end for**
 - 15: Set $\varepsilon = \sum_{i=2}^N |\varepsilon^i|$.
 - 16: **if** $\varepsilon > \tau$ **then**
 - 17: Use Broyden's method to choose new values of $c^i(s_0)$ and return to Step 3.
 - 18: **end if**
 - 19: **end while**
-

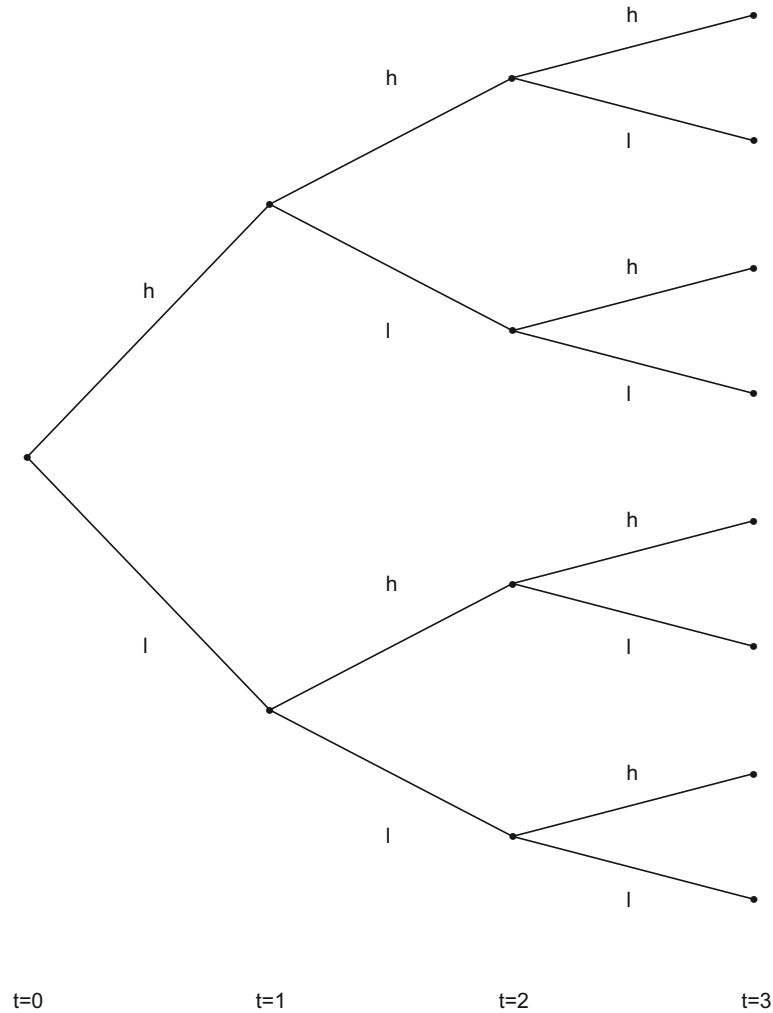


Figure 6 A state-tree diagram of the heterogeneous beliefs model for the case of $S = 2$ (l and h) and $T = 3$.

5.3 Results

Let us now consider a specialization of the model in [Section 5.1](#) with $S = 2$ and $I = 2$. We will assume that proportions of agent types are fixed through time, $\mu^i(s^t) = \mu^i$, for $i = 1, 2$, and that agents have constant relative risk aversion utility,

$$u^i(c) = \frac{c^{1-\gamma^i}}{1-\gamma^i}. \quad (28)$$

Table 3 Maximum likelihood estimates for the parameters of the aggregate consumption growth process using a hidden Markov model and quarterly consumption data between 1947 and 2010. See Aldrich (2011) for details. Standard errors are obtained from a numerical evaluation of the Hessian.

	$\alpha(s_h)$	$\alpha(s_l)$	$\pi(s_h s_h)$	$\pi(s_l s_l)$
Estimate	-0.005011	0.006222	0.9411	0.5304
Standard error	0.001146	0.001052	0.01879	0.1213

Agents receive aggregate consumption, $C(s^t)$, as their endowment in state s^t , where the two aggregate states of nature each period, s_t , represent high consumption growth and low consumption growth ($s_t \in \{s_l, s_h\}, \forall t$). In particular, we assume that aggregate consumption follows a two-state process

$$C(s^{t+1}) = g(s^{t+1})C(s^t), \quad (29)$$

where $g(s^t) = \exp(\alpha(s_t))$, $s_t \in \{s_l, s_h\}$. The values $\alpha(s_l)$ and $\alpha(s_h)$ were estimated by Aldrich (2011) using a hidden Markov model and quarterly NIPA data between 1947 and 2010. The estimates are reported in Table 3 and include estimated transition probabilities between states. In the results reported by Aldrich (2011), the majority of agents maintain beliefs that are consistent with the estimated probabilities in Table 3, while a minority of the population deviates. In particular, that paper considers cases where the minority believes $\pi(s_l | s_l)$ is one, two, and three standard errors below its maximum likelihood estimate; i.e., they are relatively optimistic. For the present development, where we are concerned with questions of computational efficiency, it is unnecessary to take a stance on the degree of belief divergence and the proportions of agents that subscribe to each view—the timing results are unchanged by these parameters.

Table 4 reports timing results for solutions of the model over increasing time horizons T using Thrust/CUDA on the Tesla C2075 and Thrust/OpenMP and all four cores of the Xeon CPU. As with the VFI problem in the previous section, the cost of initializing the CUDA runtime environment (a bit <7 s) swamps the overall solution time of the GPU for low values of T —only when $T > 20$ does the GPU solve the model in less time than the CPU. The efficiency of the multicore CPU solution then erodes very quickly: for $T = 26$ it is roughly 10 times slower than the GPU, for $T = 28$ it is 20 times slower, and for $T = 30$ it is more than 100 times slower. Clearly, as the problem scales (for $T = \{24, 26, 28, 30\}$ the number of state-tree nodes is roughly 33 million, 130 million, 530 million, and 2 billion, respectively) the relative performance of the GPU increases. These results are remarkable, especially when considering total computational efficiency of each processing unit: the Tesla C2075 is capable of 515 billion floating point operations per second (FLOPS), while the quad-core Xeon is capable of roughly 77 billion FLOPS (both measurements are for double precision arithmetic). These numbers

Table 4 Timing results (in seconds) for the heterogeneous beliefs model over increasing horizon T . “Thrust/OpenMP” and “Thrust/CUDA” refer to the Thrust implementation, using the separate backends for OpenMP (on the quad-core Xeon CPU) and CUDA (on the Tesla C2075).

T	5	10	15	20	22	24	26	28	30
Thrust/OpenMP	0.0004110	0.002138	0.04968	1.1934	6.864	35.88	113.0	461.1	7021
Thrust/CUDA	6.630	6.646	6.606	6.686	6.767	7.507	10.15	23.40	67.15

suggest that the GPU should be no more than roughly 6.5 times faster than the CPU. As suggested in Lee et al. (2010b), applying various CPU optimizations might ameliorate the results reported in Table 4. However, such optimizations would be challenging for most economists and the results of this section compare software implementations that are of commensurate difficulty and accessible to the majority of economists. In this sense, these results compare operational efficiency: they compare not only hardware, but also software implementations that require roughly the same level of technical expertise and how they interact with the hardware. As in the previous section, if we scale the solution times by processor cost at $T = 30$, the GPU is roughly 16 times more efficient (time/dollar) than the quad-core CPU. This is a substantial improvement relative to the VFI problem.

Increasing the complexity of the VFI problem in the previous section translated to greater solution accuracy; in this problem increasing complexity has no bearing on solution accuracy, but increases the time horizon for the model under question. With a quarterly calibration, $T = 20$ (which the CPU can compute quickly) and $T = 28$ (for which the CPU is much slower) correspond to horizons of 5 and 7 years. With multiple GPUs it would be feasible to push the horizon well past a decade, and with a cluster of hundreds of GPUs (such as the Titan supercomputing system at Oak Ridge National Lab: <http://www.olcf.ornl.gov/titan/>) it would be possible to extend the horizon to several decades. To the extent that important economic decisions are being made at long horizons, being able to compute such models adds real economic value to understanding agents' decisions. This is true of the model in Aldrich (2011) for which issues of survival play a role in the exchange of assets.



6. THE ROAD AHEAD

Developments in software and hardware will necessarily influence the way we design both GPU algorithms (in particular) and massively parallel algorithms (in general). The current state of the art for GPGPU computing requires algorithmic design that favors identical execution of instructions over heterogeneous data elements, avoiding execution divergence as much as possible. Occupancy (discussed in Section 2.1.3) is another important consideration when parallelizing computations: most current GPUs are only

fully utilized when the number of execution threads is on the order of 10,000–30,000. While GPU parallelism in most algorithms can be achieved in a variety of ways, these two issues, divergence and occupancy, direct scientists to parallel schemes that involve a small set of simple instructions executing on a large number of data elements. This is largely a result of the physical hardware constraints of GPUs—the number of transistors dedicated to floating point vs. memory and control-flow operations. In time, as both GPU and other massively parallel hardware changes, the design of algorithms suitable for the hardware will also change. And so, while this paper has provided some examples of algorithmic design for GPU architectures, it is most important for researchers to be aware of and sensitive to the changing characteristics of the hardware they use. The remainder of this section will highlight recent developments in parallel hardware and software and in so doing will cast our gaze to the horizon of massively parallel computing.

6.1 NVIDIA Kepler and CUDA 5

CUDA 5, the most recent toolkit released by NVIDIA on 15 October 2012, leverages the new NVIDIA Kepler architecture to increase productivity in developing GPU software. Among others, the two most notable features of CUDA 5 are dynamic parallelism and GPU callable libraries.

Dynamic parallelism is a mechanism whereby GPU threads can spawn more GPU threads directly, without interacting with a CPU. Previous to CUDA 5, all GPU threads had to be instantiated by a CPU. However, a kernel which is executed by a GPU thread can now make calls to other kernels, creating more threads for the GPU to execute. Best of all, the coordination of such threads is handled automatically by the scheduler on the GPU multiprocessor. This increases the potential for algorithmic complexity in GPU parallel algorithms, as multiple levels of parallelism can be coordinated directly on the GPU. Dynamic parallelism is only available on Kepler-capable NVIDIA GPUs released after 22 March 2012.

GPU callable libraries allow developers to write libraries that can be called within kernels written by other users. Prior to CUDA 5, all GPU source code had to be compiled within a single file. With the new toolkit, however, scientists can enclose GPU software in a static library that can be linked to third-party code. As high-performance libraries are created, this feature will extend the capabilities of individual researchers to write application-specific software, since they will be able to rely on professionally developed libraries rather than writing their own routines for each problem. An example would be simple regression or optimization routines: if an application requires such routines to be called within a GPU kernel, the new CUDA toolkit allows them to be implemented in a third-party library, rather than written personally by an individual developing the particular application. GPU callable libraries only depend on CUDA 5 and not on the Kepler architecture—older NVIDIA GPUs can make use of callable libraries so long as they have the CUDA 5 drivers installed.

GPU callable libraries and dynamic parallelism interact in a way that results in a very important feature: GPU libraries that were previously only callable from a CPU can now be called directly within a kernel. As an example, CUDA BLAS, which leverages GPU parallelism for BLAS operations, can now be called by a GPU thread in order to perform vector or matrix operations. Prior to CUDA 5, vector and matrix operations had to be written by hand if performed within a GPU kernel. This feature, of course, will extend to other GPU libraries which spawn many threads in their implementation.

6.2 Intel Phi

On 12 November 2012, Intel released a new microprocessor known as the Intel Xeon Phi ([Intel Corporation \(2013b\)](#)). To be specific the Phi is a *coprocessor* which can only be utilized in tandem with a traditional CPU that manages its operations. However, the 50 individual cores on the Phi are x86 processors in their own right, similar to x86 cores in other Intel CPU products. In other words, each Phi core possesses the capabilities of running a full operating system and any legacy software that was written for previous generation x86 CPUs.

The primary objective of the Phi is to introduce many of the advantages of GPU computing within an architecture that doesn't sacrifice the benefits of traditional CPUs. At 1.05 GHz each, the 50 Phi cores don't deliver as much raw compute power as a Tesla C2075 GPU, but they allow for far greater functionality since they have many more transistors dedicated to memory use and control flow. This effectively eliminates the issues of thread divergence and allows serial software to be more quickly and easily ported to parallel implementations. It also allows the use of third-party numerical libraries and software without modification.

It is difficult to forecast the nature of future parallel processors, but it is very likely that hybrid processors like the Xeon Phi will become increasingly relevant since they combine the benefits of GPU parallelism with the flexibility that is necessary for a wide variety of computational tasks. Future processors may also synthesize the benefits of the Phi and current GPUs by placing heterogeneous compute cores on a single, integrated chip, overcoming memory transfer issues and simultaneously allowing for greater thread divergence within a massively parallel framework.

6.3 OpenACC

OpenACC ([OpenACC \(2013\)](#)) is an example of a programming standard that allows for high-level development of parallel computation. Developed jointly by Cray, NVIDIA, and PGI, OpenACC allows users to insert compiler directives to accelerate serial C/C++ and Fortran code on parallel hardware (either a CPU or a GPU). In this way, OpenACC is very similar to OpenMP which accelerates serial code on multicore CPUs.

OpenACC is an important example of software that promotes parallelism at a very high level—it requires very little effort to extend serial code to parallel hardware. With

some sacrifice of efficiency and flexibility, OpenACC takes GPU computing into the hands of more software designers and offers a glimpse of the future of parallel computing: software which automatically incorporates the benefits of massive parallelism with very little user interaction. Coupled with future advances in hardware, this could dramatically alter the ways in which parallel algorithms are designed.



7. CONCLUSION

This paper has provided an introduction to current tools for GPU computing in economics and has demonstrated the use of these tools with examples. [Sections 4](#) and [5](#) demonstrated the benefits of GPU computing for two specific economic problems. For example, a current NVIDIA GPU intended for scientific computing was able to speed the solution of a basic dynamic programming problem by thousands of times relative to a single-threaded C++ or Matlab implementation. Relative to a multithreaded CPU solution making use of the same software library, the GPU gains were more muted: roughly 5 times. GPU parallelism was also striking in the heterogeneous beliefs model of [Section 5](#), where the model solution was 100 times faster on a GPU than a quad-core CPU for long time horizons.

Adoption of GPU computing has been slower in economics than in other scientific fields, with the majority of software development occurring within the subfield of econometrics. Examples include [Lee et al. \(2010a\)](#), [Creel and Kristensen \(2011\)](#), [Durham and Geweke \(2011\)](#), and [Durham and Geweke \(2012\)](#), all of which exploit GPUs within an MCMC or particle filtering framework. These papers demonstrate the great potential of GPUs for econometric estimation, but the examples of this paper also highlight the inherent parallelism within a much broader set of economic problems. The truth is that almost all computationally intensive economic problems can benefit from massive parallelism—the challenge is creatively finding the inherent parallelism, a task which often involves changing the way the problem is traditionally viewed or computed. This paper also provides guidance for determining if that inherent parallelism is well suited for a massively parallel GPU architecture.

The intent of the examples in this paper is to demonstrate how traditional algorithms in economics can be altered to exploit parallel resources. This type of thought process can then be applied to other algorithms. However, since the tools of massive parallelism are ever changing, so will the design of parallel algorithms. The current architecture of GPUs guides the development of parallel software since it places limitations on memory access and control flow, but as these aspects are likely to change with the development of new many-core and heterogeneous processors, the ability to perform parallel computations on many data elements will also change. The overriding objective then is to creatively adapt algorithms for new and changing architectures.

As time progresses, parallel computing tools are becoming more accessible for a larger audience. So why learn the nuts and bolts of GPU computing now? Why not wait a couple of years until it is even more accessible? For many researchers, waiting might be the optimal path. However, a frontier will always exist and pushing the frontier will not only yield returns for computationally challenging problems, but it will also inform economists' choices about paths for future research. For the economist who is tackling computationally intensive problems and is often waiting long periods of time for a computer to yield solutions, becoming fluent in the tools of this paper and staying at the frontier will pay great dividends.

REFERENCES

- Aldrich, E.M., 2011. Trading Volume in General Equilibrium with Complete Markets. Working Paper.
- Aldrich, E.M., Fernández-Villaverde, J., Gallant, A.R., Rubio-Ramírez, J.F., 2011. Tapping the super-computer under your desk: solving dynamic equilibrium models with graphics processors. *Journal of Economic Dynamics and Control* 35, 386–393.
- Amdahl, G.M., 1967. Validity of the single processor approach to achieving large scale computing capabilities. *AFIPS Conference Proceedings* 30, 483–485.
- Bell, N., Hoberock, J., 2012. Thrust: A Productivity-Oriented Library for CUDA. In: Hwu, W.-M.W. (Ed.), *GPU Computing Gems*, Chap. 26, pp. 359–372.
- Charalambous, M., Trancoso, P., Stamatakis, A., 2005. Initial Experiences Porting a Bioinformatics Application to a Graphics Processor. In: Bozaris, P., Houstis, E.N. (Eds.), Vol. 3746 of *Lecture Notes in Computer Science*, Springer-Verlag, Berlin, pp. 415–425.
- Creal, D.D. 2012. Exact Likelihood Inference for Autoregressive Gamma Stochastic Volatility Models, Working Paper, pp. 1–35.
- Creel, M., Kristensen, D. 2011. Indirect Likelihood Inference, Working Paper.
- Dongarra, J.J., van der Steen, A.J., 2012. High-performance computing systems: status and outlook. *Acta Numerica* 21, 379–474.
- Durham, G., Geweke, J., 2011. Massively Parallel Sequential Monte Carlo for Bayesian Inference, Working Paper.
- Durham, G., Geweke, J., 2012. Adaptive Sequential Posterior Simulators for Massively Parallel Computing Environments, Working Paper, pp. 1–61.
- Dziubinski, M.P., Grassi, S., 2012. Heterogeneous Computing in Economics: A Simplified Approach, Working Paper.
- Fulop, A., Li, J., 2012. Efficient Learning via Simulation: A Marginalized Resample-Move Approach, Working Paper, pp. 1–48.
- Harris, M.J., Baxter III, W.V., Scheuermann, T., Lastra, A., 2003. Simulation of cloud dynamics on graphics hardware. In: *Proceedings of Graphics Hardware*, Euro-Graphics Association, pp. 92–102.
- Heer, B., Maussner, A., 2005. *Dynamic General Equilibrium Modelling*, Springer, Berlin.
- Intel Corporation, 2011. Intel Xeon Processor E7–8800 / 4800 / 2800 Product Families, Datasheet, 1.
- Intel Corporation, 2013a. Desktop 3rd Generation Intel Core Processor Family, Desktop Intel Pentium Processor Family, and Desktop Intel Celeron Processor Family, Datasheet 1, pp. 1–112.
- Intel Corporation, 2013b. The Intel Xeon Phi Product Family, Product Brief.
- Judd, K.L., 1998. *Numerical Methods in Economics*. MIT Press, Cambridge, MA.
- Kruger, J., Westermann, R., 2002. Linear algebra operators for GPU implementation of numerical algorithms. *ACM Transactions on Graphics* 908–916.
- Kydland, F.E., Prescott, E.C., 1982. Time to build and aggregate fluctuations. *Econometrica* 50, 1345–1370.
- Lee, A., Yau, C., Giles, M.B., Doucet, A., Holmes, C., 2010a. On the utility of graphics cards to perform massively parallel simulation of advanced monte carlo methods. *Journal of Computational and Graphical Statistics* 19, 769–789.

- Lee, V.W., Kim, C., Chhugani, J., Deisher, M., Kim, D., Nguyen, A.D., Satish, N., Smelyanskiy, M., Chennupati, S., Hammarlund, P., Singhal, R., Dubey, P., 2010b. Debunking the 100X GPU vs. CPU Myth: an evaluation of throughput computing on CPU and GPU. In: Proceedings of the 37th Annual International Symposium on Computer Architecture, pp. 451–460.
- Microsoft, 2012. C ++ AMP : Language and Programming Model, Specification.
- NVIDIA, 2011. NVIDIA Tesla C2075 Companion Processor, Product Brief.
- NVIDIA, 2012a. Cuda C Programming Guide, Manual.
- NVIDIA, 2012b. Thrust Quick Start Guide v5.0, Manual.
- OpenACC, 2013. The OpenACC Application Programming Interface, Version 2.
- PCI-SIG, 2006. PCI Express 2.0 Base Specification, Specification.
- Purcell, T.J., Buck, I., Mark, W.R., Hanrahan, P., 2002. Ray tracing on programmable graphics hardware. *ACM Transactions on Graphics* 21, 703–712.
- Stokey, N.L., Lucas, R.E. Jr., Prescott, E.C., 1989. *Recursive Methods in Economic Dynamics*. Harvard University Press, Cambridge, MA.
- Stone, J.E., Phillips, J.C., Freddolino, P.L., Hardy, D.J., Trabuco, L.G., Schulten, K., 2007. Accelerating molecular modeling applications with graphics processors. *Journal of Computational Chemistry* 28, 2618–2640.
- Tauchen, G., 1986. Finite state markov-chain approximations to univariate and vector autoregressions. *Economics Letters* 20, 177–181.